ELSEVIER

Biophysical Chemistry 92 (2001) 65–75

Biophysical Chemistry

www.elsevier.com/locate/bpc

DSC studies of *Fusarium solani pisi* cutinase: consequences for stability in the presence of surfactants

Lucia D. Creveld[a,b], Wim Meijberg[c], Herman J.C. Berendsen[b], Henri A.M. Pepermans[a,*]

[a] *Unilever Research, Olivier van Noortlaan 120, 3133 AT Vlaardingen, The Netherlands*
[b] *Biophysical Chemistry, University of Groningen, Nijenborgh 4, 9747 AG Groningen, The Netherlands*
[c] *BiOMaDe, Nijenborgh 4, 9747 AG Groningen, The Netherlands*

Received 9 April 2001; received in revised form 13 June 2001; accepted 14 June 2001

Abstract

The application of cutinase from *Fusarium solani pisi* as a fat-stain removing ingredient in laundry washing is hampered by its lack of stability in the presence of anionic surfactants. We postulate that the stability of cutinase towards anionics can be improved by mutations increasing its temperature stability. Thermal unfolding as measured with DSC, appears to be irreversible, though the thermograms are more symmetric than predicted by a simple irreversible model. In the presence of taurodeoxycholate (TDOC), the unfolding temperature is lower and the unfolding is reversible. We conclude that an early reversible unfolding intermediate exists in which a number of additional hydrophobic patches are exposed to the solvent, or preferentially are covered with TDOC. Improvement of the stability of cutinase with respect to both surfactants and thermal denaturation, should thus be directed toward the prevention of exposure of hydrophobic patches in the early intermediate.

Keywords: Cutinase; Lipase; Protein stability; Protein unfolding; Surfactants; Differential scanning calorimetry (DSC)

1. Introduction

Cutinases are enzymes with a molecular mass of 22–25 kDa that hydrolyse ester bonds of the cutin polymer in the plant cell wall. They are serine esterases, which are also able to hydrolyse a wide variety of synthetic esters and triacylglycerols [1,2]. Since a cutinase is an efficient catalyst both in solution and at the water–lipid interface, it is potentially suitable for lipid stain removal applications in the detergent industry [3]. The implementation of the enzyme as a fat-stain removing ingredient in laundry washing is hampered by its unfolding in the presence of anionic surfactants. We postulate that the stability of

* Corresponding author. Tel.: +31-10-4606278; fax: +31-10-4605671.
E-mail address: rik.pepermans@unilever.com (H.A.M. Pepermans).

0301-4622/01/$ - see front matter
PII: S0301-4622(01)00187-9

cutinase towards anionics can be improved by mutations increasing its temperature stability. The structure [4–6], flexibility [7–9] and the stability (as reviewed in [10]) of *Fusarium solani pisi* cutinase have been studied extensively, which makes it particularly suitable to test this hypothesis.

The first measurements of the thermal stability of cutinase in solution showed that formation of aggregates was one of the processes leading to thermal inactivation. Aggregation decreased rapidly above pH 7, and was not affected by salt concentration or by the presence of metal ions [2]. The formation of aggregates is also found for NMR samples of cutinase above a concentration of 0.5 mM. After a delay, depending on the conditions but hard to predict precisely, the sample suddenly becomes turbid, and then the aggregate precipitates. After aggregation, 0.5 mM is still left in solution (personal communication, Anneke Groenewegen).

The first thermal stability study reported that cutinase displays activity up to 85°C [2]. Other authors found unfolding temperatures ranging from 39 to 70°C, depending on the applied method and solvent used [3,11,12]. Several studies have been performed on the immobilisation of cutinase in reversed micelles, or on solid supports [10]. Immobilisation often increases the thermostability of the enzyme as the interaction of the support with the enzyme leads to a more rigid conformation of the enzyme [13]. Moreover, immobilisation is of interest with regard to the applications to biocatalysis in organic media.

Pocalyko and Tallman [14] have studied the adverse effect of sodium dodecylsulphate (SDS — an anionic surfactant, Fig. 1) on the activity and stability of cutinase, reported earlier by Kolattukudy [1]. They suggested that SDS causes local conformational changes in the active site that result in inhibition, partial reversible unfolding, and subsequent inactivation. They showed that these changes could be reversed by the addition of Triton X-100 (non-ionic surfactant). This is accompanied by an irreversible loss of activity, more slowly than the initial loss. Similarly, Egmond et al. found that the description of the unfolding process in the presence of LDS, at concentrations above 0.5 mM, requires at least two first-order rate constants [15]. They also found that refolding can be achieved by addition of detergents that are inert towards cutinase. In addition, Egmond and van Bemmel found that the inactivation is preceded by a specific interaction between the anionic surfactant and the surface of the protein. For this process, the location of the positive charge as well as the distribution of hydrophobicity over the surface of the enzyme is important: it should be complementary to the negatively charged head group and the long, extended tail of the anionic surfactants [16]. One of the possible recognition sites is the substrate-binding site. This may explain the inhibition of cutinase by SDS, without effecting the stability.

Sodium taurodeoxycholate (TDOC, Fig. 1, CMC = 3.0 mM), an anionic surfactant with a bulky tail, has been shown to be applicable in experimental studies requiring high enzyme concentrations without aggregation. NMR T_2 relaxation measurements have been performed on TDOC in the presence and absence of native cutinase (unpublished results). The measurements indicate that in the presence of the enzyme the mobility of the hydrophobic part of TDOC is reduced more than that of the taurine moiety. This indicates that TDOC binds at hydrophobic sites of the protein.

Differential scanning calorimetry (DSC) is a powerful technique to characterise temperature-induced conformational changes in proteins [17–21]. An important advantage of this technique is that the unfolding temperature and enthalpy can be determined directly and do not have to be derived, e.g. from activity measurements using spectroscopic methods at different temperatures.

Here, we present DSC measurements for cutinase to get a better picture of the unfolding behaviour of cutinase. We will discuss why unfolding as measured by DSC is a good model for unfolding due to anionic surfactants.

2. Materials and methods

2.1. Enzyme

Recombinant cutinase was produced in *Saccharomyces cerevisiae* and purified as described

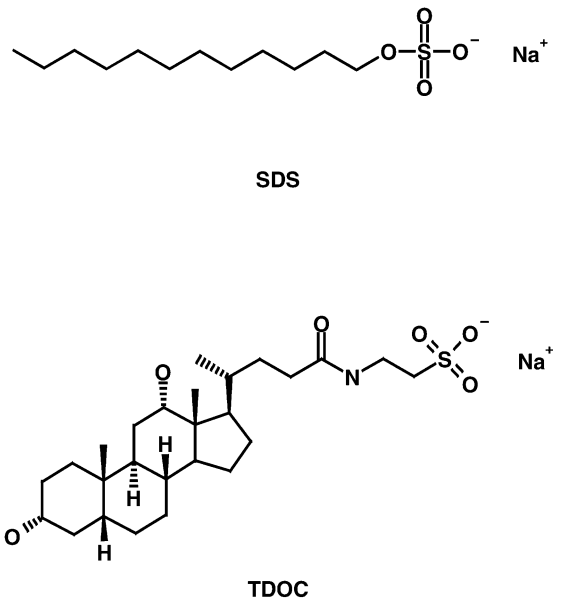

Fig. 1. Structure of sodium dodecylsulphate (SDS) and sodium taurodeoxycholate (TDOC).

previously [22,23]. The enzyme was dissolved in 10 mM Tris buffer with 40 mM NaCl at pH 9.0 at a concentration of ~ 1.0 mg ml^{-1}. Protein concentrations were determined spectrophotometrically at 280 nm, using a molar extinction coefficient of 0.713 M^{-1} cm^{-1}. The DSC measurements at different scan rates were performed with one stock solution. The measurements in the presence of taurodeoxycholate (TDOC) were performed in the same buffer with 5.0 mM Na TDOC.

2.2. Differential scanning calorimetry

All DSC measurements were performed on a MCS differential scanning calorimeter from Microcal (Northampton, MA, USA) with buffer in the reference cell under a 1.5 bar nitrogen pressure. Samples were degassed by stirring gently under vacuum prior to measurements. Protein unfolding events were recorded between 5 and 85°C with a scan rate of 1.0 K min^{-1} unless indicated otherwise, and 15 s filter time. In order to check for reversibility of the observed transitions, rescans of the samples were performed after cooling to 5°C. The scans were analysed after subtraction of an instrument baseline recorded with buffer in both cells using the software package ORIGIN (Microcal).

2.3. Simulation of irreversible models

Mathematica (Wolfram research) was used for analysis of the irreversible models. For curve fitting, only those experimental data were used that had c_p^{ex} values greater than a threshold, taken as twice the standard deviation (S.D.) calculated from points at temperatures less than 46°C. At scan rates of 0.5, 1.0 and 2.0 K min^{-1}, 88, 47 and 24 data points remained as a result of S.D.s of 0.2, 0.2 and 0.08 kJ mol^{-1} K^{-1}, respectively. The parameters were fitted by minimising simultaneously, the sum of the squared differences between the three experimental and simulated curves. The squared differences from the curve of the 2.0 K min^{-1} scan rate were given a five times larger weight than the squared differences of the curves of the two other scan rates.

3. Theory

Corrected DSC curves are expressed as the excess heat capacity per mole of protein c_p^{ex} as a function of time, measured at a given constant scan rate v. The absorbed heat $Q(T)$ is defined as the integral of c_p^{ex} from a low temperature (here 45°C) to T. The total absorbed heat over the full transition is the unfolding enthalpy ΔH. The temperature at which $Q(T) = 0.5\Delta H$ is called the apparent melting temperature T_{app} [24], the temperature at which the population of native and unfolded protein are equal if the folding process is a two-state reversible process. This is not necessarily equal to the temperature at which c_p^{ex} is maximal, which is indicated by T_{max}.

Protein unfolding can be either reversible of irreversible. The simplest realistic model which includes both possibilities comprises two steps: (1) reversible denaturation of the native protein (N) with an equilibrium constant $K_{eq} = k_1/k_2$ to yield an unfolded, or partially unfolded state (U); and (2) irreversible alteration of the (partially) unfolded state [17] with a rate constant k_3 to pro-

duce the final state (F), which is unable to fold back to the native protein. This model can be depicted as:

$$N \underset{k_2}{\overset{k_1}{\rightleftarrows}} U \overset{k_3}{\rightarrow} F \tag{1}$$

and is known as the Lumry–Eyring model [25]. The possible processes enforcing the irreversible step, like aggregation, autolysis, chemical alteration of residues, have been reviewed by Klibanov and Ahern [26,27]. Depending on the constants k_2 and k_3, two extreme cases may be identified:

$k_3 \ll k_2$: The unfolding is a two-state reversible process. Detailed information about the energetics and mechanism of unfolding can be obtained [28,29]. The Gibbs free energy ($\Delta G = G_U - G_N$) is related to the equilibrium constant K_{eq} by $\Delta G = -RT\ln K_{\mathrm{eq}}$, and may be expressed as: $\Delta G = \Delta H - T\Delta S$, where the entropy term (ΔS) favours the unfolded structure and the enthalpy term (ΔH) favours the native fold;

$k_3 \gg k_2$: The unfolding is a two-state irreversible process [30,31]. Equilibrium thermodynamics analysis is not applicable, and only the unfolding enthalpy can be measured.

3.1. Two-state reversible unfolding

The two-state reversible unfolding model is given by:

$$N \underset{k_2}{\overset{k_1}{\rightleftarrows}} U. \tag{2}$$

Experimentally, the reversibility of unfolding is verified in a rescan. For a fully reversible process, the DSC thermograms for the first scan and the rescan should show identical transitions.

The fraction unfolded protein x is proportional to the integrated heat capacity:

$$Q(T) = \Delta H \cdot x(T). \tag{3}$$

For slow scan rates, N and U are always in equilibrium and $x(T)$ is determined by the equilibrium constant $K(T)$:

$$K(T) = \frac{x}{(1-x)} = \exp\left(-\frac{\Delta G}{RT}\right). \tag{4}$$

The *apparent van't Hoff enthalpy* ΔH^{vH} can be found by plotting $\ln K(T)$ vs. $1/T$. For a fully reversible unimolecular two-state process, ΔH^{vH} equals the total absorbed heat ΔH [17], for reversible processes with intermediate states smaller values are found [32], while for irreversible processes ΔH^{vH} can be considerably larger than ΔH.

The shape of the DSC transition depends on the scan rate v when v/k, where $k = k_1 + k_2$, reaches values comparable to the width of the transition. From the rate equations it follows that

$$x = x_{\mathrm{eq}} - \left(\frac{v}{k}\right)\frac{\mathrm{d}x}{\mathrm{d}T}. \tag{5}$$

This implies that the transition curves shift from the ideal equilibrium curve ($v = 0$) to higher temperatures, for small scan rates approximately as:

$$x(T) = x_{\mathrm{eq}}\left(T + \frac{v}{k}\right). \tag{6}$$

The shift should be proportional to v. Because of the temperature dependence of k the curves also become steeper and the apparent van't Hoff heats increase with v.

3.2. Two-state irreversible unfolding

The two-state irreversible model is given by:

$$N \overset{k}{\rightarrow} F \tag{7}$$

where the first-order rate constant k can be identified with k_1 of Eq. (1). In this case all molecules in the native state are irreversibly unfolded into the final state. The total absorbed heat now equals the enthalpy change from N to F; it is generally assumed that the enthalpy change from U to F is negligible compared to that from N to U.

A sensitive test of this model is the derivation of $k(T)$ from scans at various scan rates. From the kinetic equation one derives [30]:

$$k(T) = \frac{vc_p^{ex}(T)}{\Delta H - Q(T)}. \quad (8)$$

For this model to hold, there must be agreement between the values of k calculated from DSC transitions obtained at different scan rates. Plotting $\ln k$ vs. $1/T$ should yield overlapping curves with the same slope, from which an *apparent activation energy* can be derived.

The shape of the DSC transition follows from integration of the kinetic equation and is given by [31]:

$$c_p^{ex} = \frac{k(T)\Delta H}{v} \exp\left(-\frac{1}{v} \int_{T_0}^{T} k(T) dT \right). \quad (9)$$

Assuming Arrhenius behaviour for $k(T)$, this equation can be used to simulate the curves for comparison with experiment.

4. Results and discussion

4.1. Unfolding behaviour of cutinase

Fig. 2 shows the DSC transition of *Fusarium solani pisi* cutinase. This thermogram was recorded at a pH of 9.0 in 10 mM Tris buffer and 40 mM NaCl, a protein concentration of 1.0 mg ml^{-1} and a scan rate of 1.0 K min^{-1}. Under these conditions the T_{max} of cutinase is 54.4°C. At temperatures above 65°C a strongly exothermic process is observed, which is likely to be due to aggregation and precipitation of unfolded protein. The unfolding process is completely irreversible, as is evident from the rescan after heating to 61°C, shown in the insert of Fig. 2, and from the turbidity of the sample after heating. If a rescan from T_{max} is performed, a similarly shaped thermogram is measured where the apparent enthalpy is halved, corresponding to the unfolding of the half of the molecules not irreversibly unfolded in the first scan.

The T_{max} for this experiment is higher than the one of 50.1°C at a pH of 9.6 determined through UV absorbance measurements, with a protein concentration of 0.67 mg ml^{-1} and lower scan rate [11]. This difference can be readily explained, as the unfolding temperature of proteins depends strongly on the pH, the salt concentration in solution and the scan rate at which the measurements have been carried out. Petersen et al. mea-

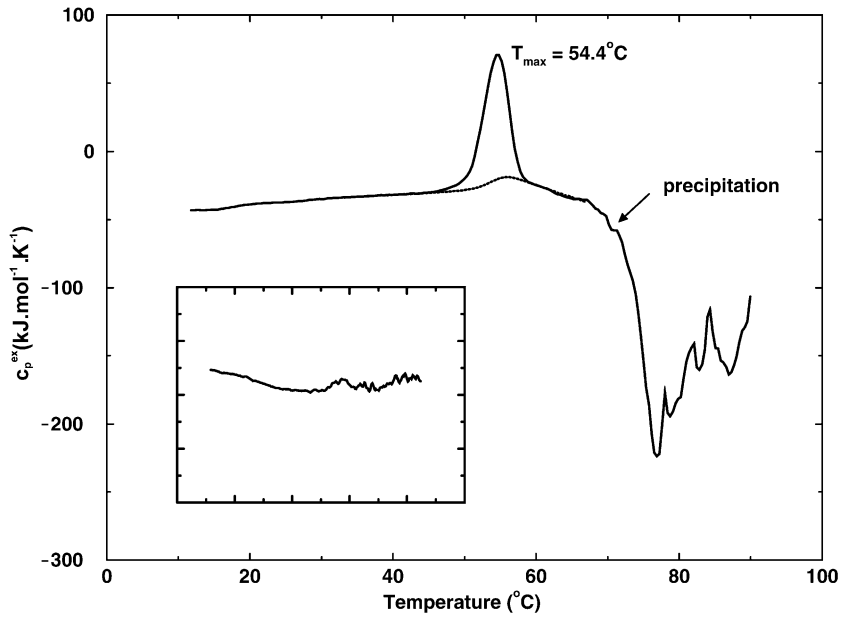

Fig. 2. DSC transition for *Fusarium solani pisi* cutinase; the inset shows a rescan from a sample that was cooled down from 61°C.

Table 1
Properties of the baseline-corrected scans of *Fusarium solani pisi* cutinase at three scan rates and in the presence of TDOC

Scan rate (K/min)	T_{max} (°C)	T_{app} (°C)	ΔH (kJ mol^{-1})	ΔH^{vH} (kJ mol^{-1})
0.5	53.4	53.3	398	910
1.0	54.3 ± 0.2	54.2 ± 0.3	434 ± 17	888 ± 64
2.0	55.2	55.1	443	840
1.0 in the presence of TDOC	47.5	46.6	386	510

sured T_{max} as a function of pH and found an optimum T_{max} at a pH of approximately 8.8 [12]. Activity measurements at a pH of 7.5 and a concentration of 0.1 mg ml^{-1}, indicated that the enzyme is stable up to 70°C [3] or even up to 85°C [2]. In general, the use of activity measurements is expected to yield higher values for T_{max}, because actually stability of the protein–substrate complex is measured.

Melo et al. [11] also found irreversible unfolding, but they did not find aggregation despite the fact that they did their determinations with a comparable protein concentration. This difference can be explained by the experimental set-up, or the use of cutinase produced in *E. coli*. The extra *N*-terminal tail of that construct [2] lowers the protein's tendency towards aggregation (personal communication, Anneke Groenewegen). Using UV-VIS and polarisation–fluorescence measurements, aggregation of cutinase without the tail was observed directly (personal communication, Hans Meder).

Fig. 3 shows the baseline-corrected scans at three scan rates. Table 1 summarises some properties of these scans, including the *apparent van't Hoff enthalpies* of each curve. The values of ΔH should be the same for the three scans; the differences are probably due to the arbitrariness

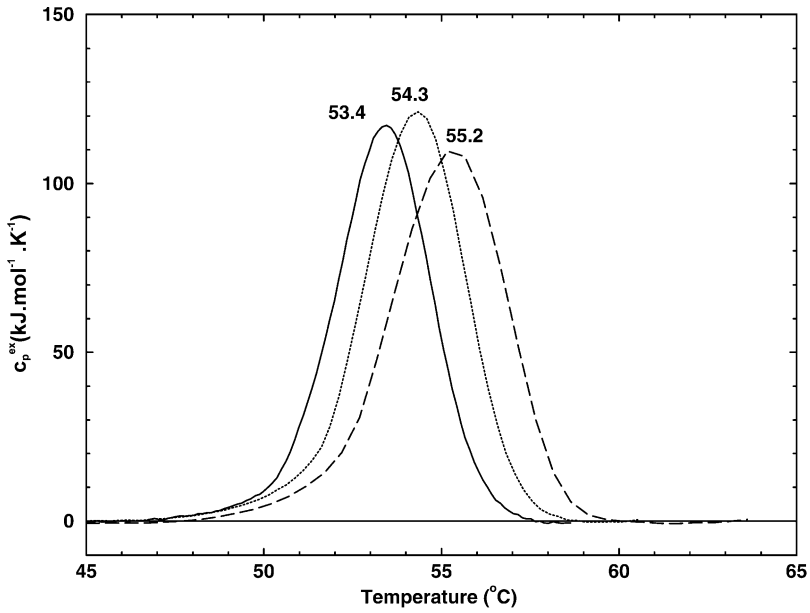

Fig. 3. DSC transitions for *Fusarium solani pisi* cutinase at three different scan rates: 0.5 (full line); 1.0 (dotted line); and 2.0 K min^{-1} (dashed line).

of the baseline correction. Both the asymmetric shape of the thermograms and the displacement of the T_{max} with different scan rates show that thermal unfolding is under kinetic control. This is in agreement with the measurements done by Petersen and co-workers [12]. The *apparent van't Hoff enthalpies* are more than twice as large as ΔH and do not increase with scan rate. This is inconsistent with any reversible model.

The observed irreversibility leaves a two-state irreversible model [Eq. (7)] as the simplest model. A first test of this model is that $k(T)$ should follow Eq. (8) at all scan rates. This is shown in Fig. 4, where $k(T)$ is plotted logarithmically vs. the reciprocal absolute temperature. There is a reasonable overlap of the three curves. The fitted line corresponds to

$$k(T) = k_0 \cdot \exp\left(-\frac{E_{app}}{R}\left(\frac{1}{T} - \frac{1}{T_0}\right)\right) \quad (10)$$

with $k_0 = 3.5 \times 10^{-4}$ min^{-1} for $T_0 = 318$ K, and $E_{app} = 670$ kJ mol^{-1}. This seems in agreement with a two-state irreversible model, but if we plot the theoretical melting curves for this process [Eq. (9)], we find that the experimental curves are more symmetric than the theoretical ones (Fig. 5). Values arrived at for the best fit were $\Delta H = 416$ KJ mol^{-1}, $k_0 = 4.0 \times 10^{-4}$ and $E_{app} = 678$ KJ mol^{-1}. The simulated curves are too asymmetric, even if fitted one by one rather than the three together, indicating that the process is more complex than a simple first-order two-state irreversible process. It is likely that a partly reversible intermediate unfolded state exists. If the exothermic reaction that takes place during the unfolding, as suggested from the increase of ΔH with increasing scan rates in Table 1, is included in curve fitting, then the shape of the curve is even harder to fit to the experimental data. In assessing the validity of the model, it should be realised that the accuracy of the tails of the $c_p^{ex}(T)$ curves is rather low because of the arbitrariness of the baseline correction. This applies

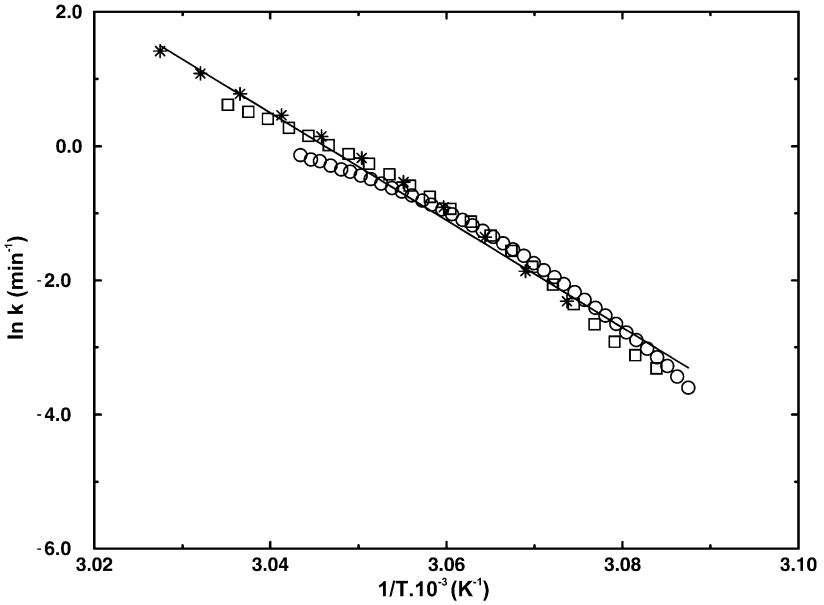

Fig. 4. The Arrhenius plot for *Fusarium solani pisi* cutinase at three different scan rates. Experimental values are indicated for 0.5 circles, 1.0 (squares), and 2.0 K min^{-1} (stars). The full line corresponds to a least square fit to all the experimental value. At the three scan rates only k values corresponding to the thermal effects higher than 5% or lower than 95% of the total unfolding heat were used to limit the effect of the relative higher uncertainty at the beginning and the end of the transition.

in particular to the high T-tail, which is influenced by the onset of the thermal effects of aggregation.

We therefore conclude that the unfolding process is more complex and involves at least one intermediate state as in the Lumry–Eyring model. The most likely situation is that there is reversible unfolding to an intermediate state, which is subject to a further irreversible process. Measurement at two times lower concentration gave the same results within experimental error (not shown), in line with the process being unimolecular. The first intermediate state is probably a short living state near to the native state, as it is not visible in the thermograms and because a rescan from the T_{max} shows that all the unfolded molecules are already irreversibly unfolded. The irreversible process will be followed by an aggregation process, which leads to a more complex reaction than the Lumry–Eyring model. Furthermore, the unfolding is complicated by the fast aggregation of the irreversible unfolded state.

4.2. Unfolding in the presence of TDOC

When 5.0 mM TDOC is added to the cutinase solution before heating, the transition temperature decreases to 47.5°C (see Fig. 6 and Table 1). TDOC apparently stabilises the unfolded state relative to the folded state. The process is completely reversible when the sample is cooled down directly after reaching 55°C, but not when the maximum temperature during the measurement is higher. The ΔH of the unfolding is comparable with the measurements without TDOC, the ΔH^{vH} is, however, lower compared to the previous measurement but still larger than ΔH, indicating that the process is not a unimolecular two-state reversible process. The difference between the T_{max} and T_{app} also indicates that the process is not a unimolecular two-state reversible unfolding. Here, TDOC probably slows down the irreversible unfolding of the unfolded molecules, allowing them to fold back into the native structure. Above 55°C the process becomes partly irreversible. In none

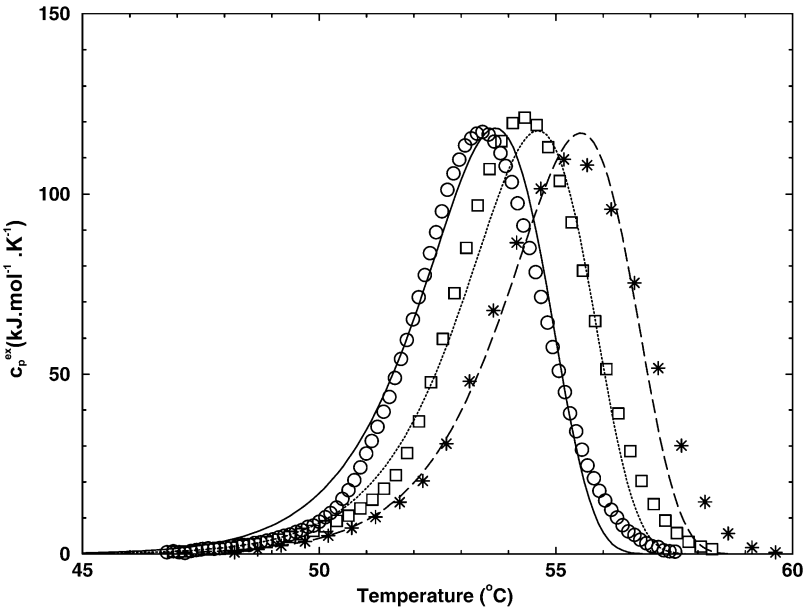

Fig. 5. Simulated curves (lines) assuming a two-state irreversible model and experimental data (symbols) for DSC transitions of *Fusarium solani pisi* cutinase at different scan rates. The lines and symbols are defined as in Figs. 3 and 4.

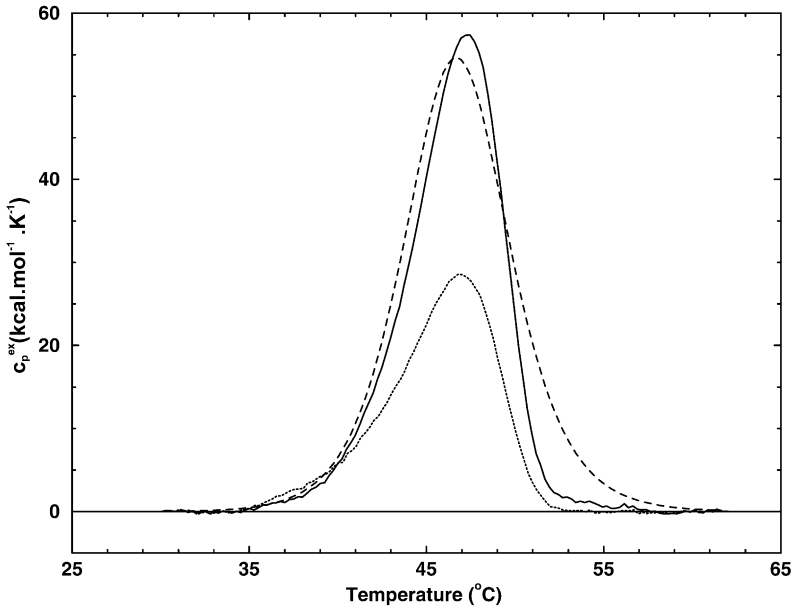

Fig. 6. DSC transition for *Fusarium solani pisi* cutinase in 5.0 mM TDOC (full line), and a rescan of the same sample which is cooled down from 85°C (dotted line). The scan rate is 1 K min^{-1}. A simulated curve assuming a two-state reversible model is included (dashed line).

of these experiments, aggregation is visible as turbidity in the sample. Probably another irreversible process than the aggregation without TDOC takes place, e.g. the coalescence of micelles.

Fig. 6 displays, together with the experimental thermogram, the theoretical melting curve for a two-state reversible process. Again, it shows that the experimental curve is less symmetric than the theoretical one. The shape of the curve may be explained by the co-operative process that takes place by the binding of TDOC at extended hydrophobic patches, which are present at the surface of the unfolded molecules.

5. Conclusion

The simplest mechanism of unfolding for cutinase in accordance with the experimental data is:

$$N \rightleftarrows [U_1] \rightarrow U_2 \rightarrow \rightarrow \text{aggregate}. \qquad (11)$$

The native state (N) irreversibly unfolds to state U_2 with a short-living on track intermediate unfolded state U_1. The unfolded state U_2 subsequently, aggregates to a final state. The thermograms show only the transition of U_1 to U_2. The unfolded state U_1 is a short living state and is near to the native state as it is only indirectly inferred from the thermograms. We have not been able to detect this intermediate by neither DSC, CD, fluorescence or NMR (unpublished data).

In the presence of TDOC, the unfolding temperature is lower and the formation of U_2 becomes reversible. Above 55°C, the unfolding remains irreversible. The simplest unfolding mechanism for cutinase in the presence of TDOC is thus:

$$N \rightleftarrows [U_1] \rightleftarrows U_2 \xrightarrow{>55^\circ C} F. \qquad (12)$$

In all states the protein is interacting with a number of TDOC molecules, which is not necessarily the same. The early intermediate U_1 is relatively more stabilised by this than U_2, as shown

by the lower value of ΔH. However, the transition state between them is even more stabilised than U_1, as indicated by the lower T_m. Apparently its stabilisation with respect to U_2 is large enough to yield a substantial backward reaction.

In the same vein, interaction of both intermediates and the transition state with SDS or SDS/Triton X-100 mixtures will alternate their relative stabilities. Moreover, the binding of SDS in the lipid binding site may give inhibition, but also stabilisation against unfolding.

Though this work did not elucidate all details of cutinase unfolding, it showed the existence of an early intermediate. It is most likely that this differs from the native state by loosening one or more loops at the surface, creating additional hydrophobicity.

The avalanche-type aggregation of the protein at high concentrations can be explained by the coalescence of hydrophobic patches of colliding molecules of the unfolding intermediate U_1. As the latter state is near to native state, a certain fraction of the molecules will be in that state at temperatures lower than T_m. As soon as two molecules dimerise, the unfolded state of the molecules gets locked. It other patches are exposed in this dimer, it forms the nucleus for the further aggregation process. At higher concentrations, the concentration of U_1 is higher too, collisions are more frequent and hence, the chance of forming dimers increases.

The first step in the mechanism of unfolding in the presence of surfactants or by increased temperature is similar; exposure of additional hydrophobic surface, which gives rise to attractive interactions with surfactants or other unfolded molecules at high concentration, and eventually to unfolding.

Improvement of the stability of *Fusarium solani pisi* cutinase might be achieved by mutations designed to avoid the transient formation of the hydrophobic patches during the motion of the protein. Insight into the internal mobility of the protein on an atomic level is obtained from molecular dynamics (MD) computer simulations [9]. To obtain the early intermediate U_1 in a significant part of the MD runs, one would like to simulate a system where it is populated significantly, like in the presence of a surfactant like TDOC. As it is not straightforward to simulate the enzyme in the presence of anionic surfactants, in computer simulations this mechanism can be mimicked by making the interactions between hydrophobic groups and solvent molecules slightly more favourable [9]. This will increase the hydrophobicity at the surface of the molecule, thus increasing the chance of unfolding during the simulation. By monitoring the transient formation of hydrophobic patches, the regions where the unfolding starts are identified and variants can be designed to prevent this.

Acknowledgements

We thank Anneke Groenewegen, Hans Meder and Hans Peters for their help with the supplementary experiments, Gea Schuurman-Wolters for her help with the DSC experiments, Jacob de Vlieg for stimulating discussions, and Carlo van Mierlo and Yves Bollen for sharing their results prior to publication.

References

[1] P.E. Kolattukudy, Cutinases from fungi and pollen in: B. Borgström, H.L. Brockman (Eds.), Lipases, Elsevier, Amsterdam, 1984, pp. 471–504.

[2] M. Lauwereys, P. de Geus, J. de Meutter, P. Stanssens, G. Matthyssens, Cloning, expression and characterization of cutinase, a fungal lipolytic enzyme in: L. Alberghina, R.D. Schmid, R. Verger (Eds.), Lipases — Structure, Mechanism and Genetic Engineering, vol. 16, VCH, Weinheim, Germany, 1991, pp. 243–251.

[3] P. de Geus, M. Lauwereys, G. Matthyssens, Cutinase, World Patent WO 90/09446, 1990.

[4] C. Martinez, P. de Geus, M. Lauwereys, G. Matthyssens, C. Cambillau, *Fusarium solani* cutinase is a lipolytic enzyme with a catalytic serine accessible to solvent, Nature 356 (1992) 615–618.

[5] S. Longhi, M. Czjzek, V. Lamzin, A. Nicola, C. Cambillau, Atomic resolution (1.0 Å) crystal structure of *Fusarium solani* cutinase: stereochemical analysis, J. Mol. Biol. 268 (1997) 779–799.

[6] J.J. Prompers, A. Groenewegen, R.C. Schaik, H.A.M. Pepermans, C.W. Hilbers, ^{1}H, ^{13}C, and ^{15}N resonance assignments of *Fusarium solani pisi* cutinase and preliminary features of the structure in solution, Protein Sci. 6 (1997) 2375–2384.

[7] J.J. Prompers, A. Groenewegen, C.W. Hilbers, H.A.M. Pepermans, Backbone dynamics of *Fusarium solani pisi* cutinase probed by nuclear magnetic resonance: the lack of interfacial activation revisited, Biochemistry 38 (1999) 5315–5327.

[8] S. Longhi, A. Nicolas, L. Creveld et al., Dynamics of *Fusarium solani pisi* cutinase investigated through structural comparison among different crystal forms of its variants, Proteins 26 (1996) 442–458.

[9] L.D. Creveld, A. Amadei, R.C. van Schaik, H.A.M. Pepermans, J. de Vlieg, H.J.C. Berendsen, Identification of functional and unfolding movements of cutinase as obtained from molecular dynamics computer simulations, Proteins 33 (1998) 253–264.

[10] D.M.L. Carvalho, M.R. Aires-Barros, J.M.S. Cabral, Cutinase: from molecular level to bioprocess development, Biotechnol. Bioeng. 66 (1999) 17–34.

[11] E.P. Melo, M.R. Aires-Barros, S.M.B. Costa, J.M.S. Cabral, Thermal unfolding of proteins at high pH range studied by UV absorbance, J. Biochem. Biophys. Methods 34 (1997) 45–59.

[12] S.B. Petersen, P.H. Jonson, P. Fojan et al., Protein engineering the surface of enzymes, J. Biotechnol. 66 (1998) 11–26.

[13] W. Norde, T. Zoungrana, Surface-induced changes in the structure and activity of enzymes physically immobilized at solid/liquid interfaces, Biotechnol. Appl. Biochem. 28 (1998) 133–143.

[14] D.J. Pocalyko, M. Tallman, Effect of amphipaths on the activity and stability of *Fusarium solani pisi* cutinase, Enzyme Microbiol. Technol. 22 (1998) 647–651.

[15] M.R. Egmond, C.J. van Bemmel, Impact of structural information on understanding lipolytic function, Methods in Enzymology 284 (1997) 119–129.

[16] M.R. Egmond, H.T.M van de Hijden, W. Musters, H. Peters, C.T. Verrips, J. de Vlieg, Modified cutinases, DNA, vector and host, World Patent WO 94/14964, 1994.

[17] A.M. Klibanov, Stabilization of enzymes against thermal inactivation, Adv. Appl. Microbiol. 29 (1983) 1–28.

[18] J.M. Sanchez-Ruiz, Differential scanning calorimetry of proteins, Subcell. Biochem. 24 (1995) 133–176.

[19] G.E. Plum, K.J. Breslauer, Calorimetry of proteins and nucleic acids, Curr. Opin. Struct. Biol. 5 (1995) 682–690.

[20] P.L. Privalov, S.A. Potekhin, Scanning microcalorimetry in studying temperature-induced changes in proteins, Methods Enzymol. 131 (1986) 4–51.

[21] J.M. Sturtevant, Biochemical application of differential scanning calorimetry, Annu. Rev. Phys. Chem. 38 (1987) 463–488.

[22] I.A. van Gemeren, W. Musters, C.A.M.J.J. van den Hondel, C.T. Verrips, Construction and heterologous expression of a synthetic copy of the cutinase cDNA of *Fusarium solani pisi*, J. Biotechnol. 40 (1995) 155–162.

[23] A. Nicolas, M.R. Egmond, C.T. Verrips et al., Contribution of cutinase serine 42 side chain to the stabilization of the oxyanion transition state, Biochemistry 35 (1996) 398–410.

[24] J.R. Lepock, K.P. Ritchie, M.C. Kolios, A.M. Rodahl, K.A. Heinz, J. Kruuv, Influence of transition rates and scan rate on kinetic simulations of differential scanning calorimetry profiles of reversible and irreversible protein denaturation, Biochemistry 31 (1992) 12706–12712.

[25] R. Lumry, H. Eyring, Conformation changes of proteins, J. Phys. Chem. 58 (1954) 110–120.

[26] A.M. Klibanov, T.J. Ahern, Thermal stability of proteins in: D.L. Oxender, C.F. Fox (Eds.), Protein Enzymology, Alan R. Liss, New York, 1987, pp. 213–218.

[27] T.J. Ahern, A.M. Klibanov, Analysis of processes causing thermal inactivation of enzymes, Meth. Biochem. Anal. 33 (1987) 91–127.

[28] K.A. Dill., Thermal stabilities of globular proteins, Biochemistry 28 (1989) 5439–5449.

[29] P.L. Privalov, Stability of proteins. Proteins which do not present a single co-operative system, Adv. Protein Chem. 35 (1982) 1–104.

[30] J.M. Sanchez-Ruiz, J.L. Lopez-Lacomba, M. Cortijo, P.L. Mateo, Differential scanning calorimetry of the irreversible thermal denaturation of thermolysin, Biochemistry 27 (1988) 1648–1652.

[31] J.M. Sanchez–Ruiz, Theoretical analysis of Lumry–Eyring models in differential scanning calorimetry, Biophys. J. 61 (1992) 921–935.

[32] L.A. Marky, K.J. Breslauer, Calculating thermodynamic data for transitions of any molecularity from equilibrium melding curves, Biopolymers 26 (1987) 1601–1620.